Comput Geosci (2007) 11:103–115
DOI 10.1007/s10596-006-9033-7

ORIGINAL PAPER

CO_2 leakage through an abandoned well: problem-oriented benchmarks

Anozie Ebigbo · Holger Class · Rainer Helmig

Received: 24 August 2006 / Accepted: 19 October 2006 / Published online: 19 December 2006

Abstract The efficiency and sustainability of carbon dioxide (CO_2) storage in deep geological formations crucially depends on the integrity of the overlying cap-rocks. Existing oil and gas wells, which penetrate the formations, are potential leakage pathways. This problem has been discussed in the literature, and a number of investigations using semi-analytical mathematical approaches have been carried out by other authors to quantify leakage rates. The semi-analytical results are based on a number of simplifying assumptions. Thus, it is of great interest to assess the influence of these assumptions. We use a numerical model to compare the results with those of the semi-analytical model. Then we ease the simplifying restrictions and include more complex thermodynamic processes including sub- and supercritical fluid properties of CO_2 and non-isothermal as well as compositional effects. The aim is to set up problem-oriented benchmark examples that allow a comparison of different modeling approaches to the problem of CO_2 leakage.

Keywords benchmarks · CO_2 sequestration · non-isothermal effects · numerical modeling · semi-analytical solutions

A. Ebigbo · H. Class (✉) · R. Helmig
Institut für Wasserbau, Lehrstuhl für Hydromechanik und Hydrosystemmodellierung, Universität Stuttgart, Pfaffenwaldring 61, 70569 Stuttgart, Germany
e-mail: holle@iws.uni-stuttgart.de

1 Introduction

The high concentration of the *greenhouse gas* carbon dioxide in the atmosphere due to the increased burning of fossil fuels has been made mainly responsible for global warming. Researchers in various disciplines are working on ways to mitigate the atmospheric carbon problem. One of the options currently discussed is the capture of CO_2 from large point sources such as fossil-fueled power plants and its storage in geological formations. Such a technology is intended to bridge the gap over the next decades until renewable capacities have been built up to fully replace the fossil energy resources. Although the time for finding solutions is rather limited, there is a vast number of scientific and political questions to work on before the carbon capture and storage technology can be applied on a scale that is significant for this global problem. One of the key issues is to find suitable target formations in which the CO_2 can be stored safely for several centuries.

The formations should be deep enough to keep the CO_2 in a liquid or supercritical state. The density of the liquid or supercritical CO_2 at such depths can vary between 250 and 750 kg/m^3. It is less dense than the resident water (brine) and thus, driven by buoyancy forces, rises towards the top of the formation. An aquitard (cap-rock) is necessary to act as a hydraulic barrier for the CO_2 plume, preventing it from further rise into shallower regions where it may be a threat to drinking water resources or even escape into the atmosphere. If the CO_2 can be kept in the formations long enough, the risk of escape is reduced by ongoing dissolution into the resident water or an immobilization by geochemical reactions with the rock.

The storage potentials of various underground formations are discussed in [15]. Deep saline aquifers are commonly assumed to be one of the most important formations because of their world-wide availability and generally low economic value. It appears to be attractive to use the existing infrastructure of oil and gas wells to inject the CO_2 into a formation. However, formations that have been explored for oil and gas production are typically perforated by a large number of wells, a fact that increases the risk of leakage through such wells. Gasda et al. [12] described this problem in detail for the deep saline Viking Aquifer in the mature sedimentary Alberta Basin in Canada where more than 300,000 wells have been drilled so far, distributed over an area of 900,000 km^2. Leakage conduits, particularly in old abandoned wells, can be manifold and include fractures in the cement plugs, corroded casings, etc.

Therefore, it is important to quantify potential leakage rates through abandoned wells and the subsequent spreading of CO_2 in overlying formations. Mathematical and numerical models for simulating the relevant physical processes are indispensable tools. For example, [19–21] presented in a series of papers the development of a semi-analytical model for investigating the CO_2 plume evolution and the leakage through abandoned wells. They set up example problems and quantified arrival times at the wells, leakage rates through the wells and discussed the influence of geometry, boundary conditions and other parameters. Simplifying assumptions were used to reduce the complexity of the equations. These include constant supercritical fluid properties, neglection of mutual solubilities and non-isothermal effects. Although such semi-analytical solutions are fast and efficient tools to solve certain problems, it is also necessary to quantify the influence of the chosen simplifications. Numerical simulators can generally solve more complex partial differential equations describing the physics more realistically, but with an accuracy that depends both on the discretization methods and meshing in space and time and on the implementation of the constitutive relationships. In recent years, a lot of research work dealt with the numerical simulation of CO_2 injection processes into geological formations [4, 22, 24, 25]. The more complex the implemented thermodynamic processes like varying fluid properties, mutual solubilities or non-isothermal effects, the more important is a verification and validation of the codes. However, this appears to be hardly feasible because reliable experimental data or field data under controlled conditions are practically not available. Thus, it is important that at least intercomparisons of the different models, both numerical and analytical ones, can be made by means of properly defined benchmark problems (see figure 1).

In this paper, we suggest a benchmark problem related to the CO_2 plume evolution and leakage through

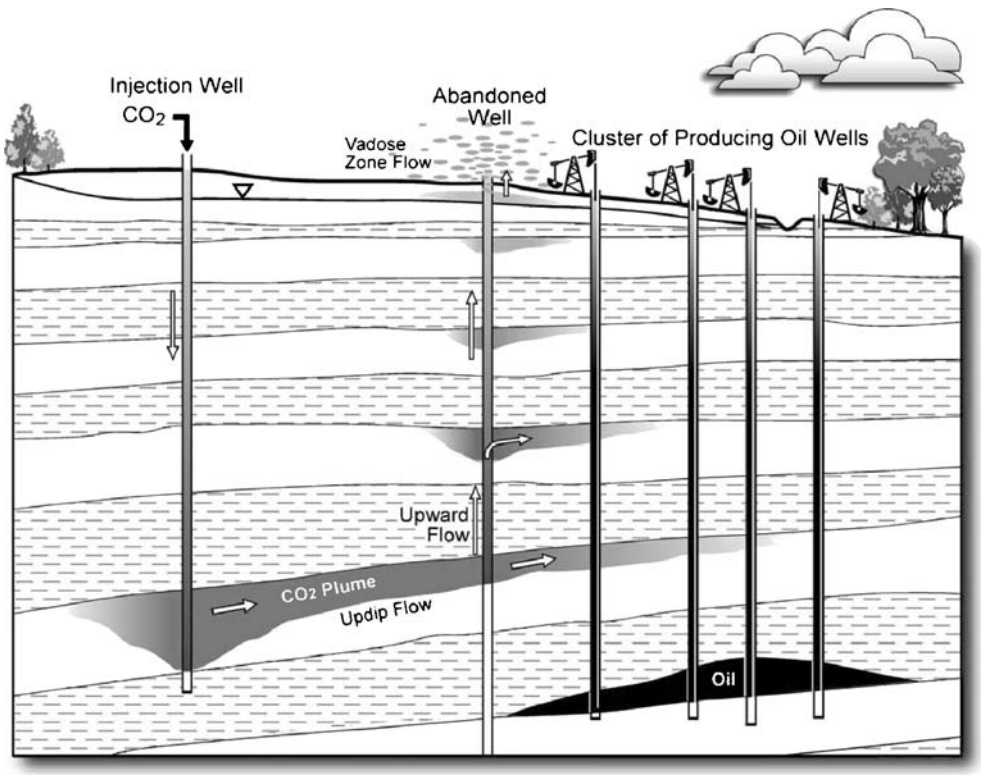

Figure 1 Typical situation of a possible injection scenario into a saline aquifer: CO_2 injection wells and producing oil wells in direct vicinity. Picture from [12].

an abandoned well using the papers of [19–21] as a reference. With this benchmark, we pursue two aims. One is to strengthen the confidence in numerical and mathematical models, but also to improve the basic understanding of the relevant physical processes by analyzing the influence of simplifications. We structure the paper as follows. After this introduction, we present a semi-analytical reference problem by summarizing the slightly modified problem suggested by [21]. We present a comparison with the results of our numerical simulator [4] using the (as far as possible) same model parameters and assumptions. We then go one step further and ease the restrictions of the model by adding more complexity to the governing equations. We include mutual solubilities and non-isothermal effects and consider also a geological formation that lies in the range of the critical depth so that the CO_2 changes from the supercritical to the subcritical state during the leakage through the wells. This puts high demands to the implementations of the required constitutive relations and is planned to act as a benchmark example also for other codes that are capable of describing this complexity.

2 The isothermal two-phase problem

2.1 The semi-analytical reference problem

2.1.1 Reference problem

A simple leakage scenario involving one CO_2 injection well, one leaky well, two aquifers and an aquitard has been set up as shown in figure 2. The leaky well connects the two aquifers. CO_2 is injected into and spreads in the lower aquifer, comes in contact with the leaky well and rises to the higher aquifer. The advective flow (including the buoyancy effects) of CO_2 in the originally brine-filled aquifers and through the leaky well is the most important process in this problem. The model domain is located 2,840 to 3,000 m below the surface and has the following dimensions: 1,000 × 1,000 × 160 m. The distance between the injection and the leaky well is 100 m, and the injection rate of CO_2 into the lower aquifer is constant. The leaky well is treated as a porous medium with a higher permeability than the formation.

This reference problem corresponds to the leakage scenario defined in [21], but on a smaller scale.

2.1.2 Assumptions/simplifications

- Fluid properties such as density and viscosity are constant.
- All processes are isothermal.
- CO_2 and brine are two separate and immiscible phases. Mutual dissolution is neglected.
- The pressure conditions at the lateral boundaries are constant over time.
- The formation is isotropic.
- Capillary pressure is negligible.

2.1.3 Semi-analytical solution

Nordbotten et al. [21] presented a semi-analytical solution procedure for the prediction of the CO_2 plume evolution during CO_2 injection into a deep saline aquifer and leakage through an abandoned well. Using the procedure, one can calculate the saturation and pressure in the formation. The CO_2 flux through the

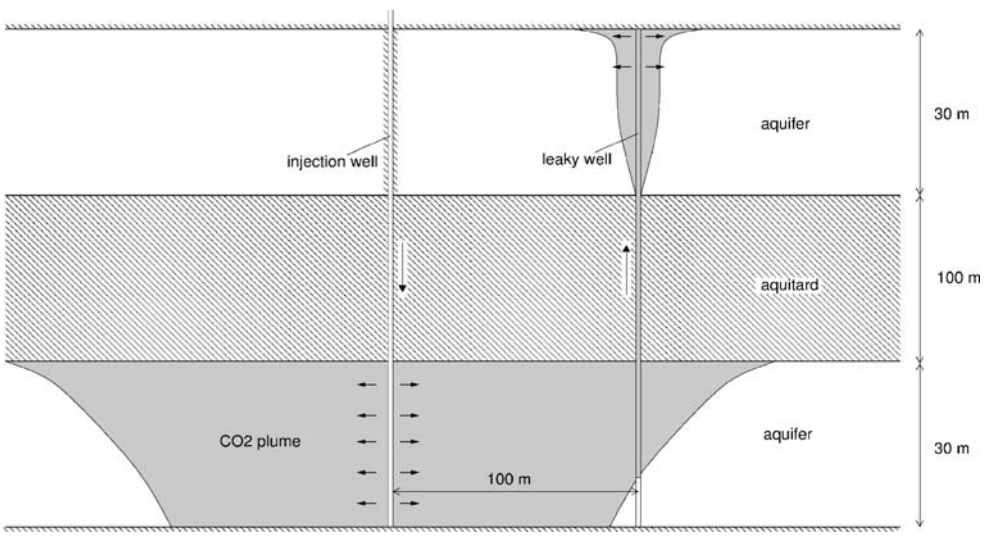

Figure 2 Leakage scenario.

leaky well is calculated using the multiphase version of Darcy's law, given the relative and absolute permeabilities in the well and the pressures in the aquifers above and below the well. This procedure has been used to calculate the leakage through the leaky well in the problem described in Section 2.1.1.

2.2 Numerical simulation

2.2.1 Governing equations and model parameters

The problem described in Section 2.1.1 has also been simulated numerically using the multiphase simulator MUFTE-UG (multiphase flow transport and energy model on unstructured grids) [1, 14]. CO_2 and brine are assumed to be two separate phases flowing through a porous medium. Mass balances of the two phases and the use of the multiphase version of Darcy's law give (with the assumptions given in Section 2.1.2) the following system of two-phase flow differential equations:

$$\begin{aligned} -\phi\frac{\partial S_\mathrm{g}}{\partial t} - \nabla\cdot\left\{\lambda_\mathrm{w}\mathbf{K}\cdot(\nabla p - \varrho_\mathrm{w}\mathbf{g})\right\} - q_\mathrm{w} &= 0 \\ \phi\frac{\partial S_\mathrm{g}}{\partial t} - \nabla\cdot\left\{\lambda_\mathrm{g}\mathbf{K}\cdot(\nabla p - \varrho_\mathrm{g}\mathbf{g})\right\} - q_\mathrm{g} &= 0 \end{aligned} \quad (1)$$

which is constrained by the equation

$$S_\mathrm{w} + S_\mathrm{g} = 1. \quad (2)$$

The primary variables in Eq. 1 are gas phase saturation S_g and pressure p. S_w is the brine phase saturation. $\lambda_\mathrm{w} = \frac{k_\mathrm{rw}}{\mu_\mathrm{w}}$ and $\lambda_\mathrm{g} = \frac{k_\mathrm{rg}}{\mu_\mathrm{g}}$ are the mobilities of the brine and gas phases, respectively. The relative permeabilities k_rw and k_rg are linear functions of S_w and S_g ($k_\mathrm{rw} = S_\mathrm{w} = 1 - S_\mathrm{g}$; $k_\mathrm{rg} = S_\mathrm{g}$). $\mathbf{g}$ is the gravity vector, $\mathbf{K}$ is the absolute permeability tensor and q_w, q_g are sources/sinks. The subscripts w and g stand for brine (water) phase and CO_2 (gas) phase, respectively. The relevant parameters used for the simulation are given in table 1.

Table 1 Simulation parameters.

Parameter	Value
CO_2 density, ϱ_g	479 kg/m^3
Brine density, ϱ_w	1,045 kg/m^3
CO_2 viscosity, μ_g	3.950×10^{-5} Pa s
Brine viscosity, μ_w	2.535×10^{-4} Pa s
Aquifer permeability, K_A	2×10^{-14} m^2
Aquifer thickness	30 m
Aquitard thickness	100 m
Leaky well permeability, K_L	1×10^{-12} m^2
Porosity, ϕ	0.15
Leaky & injection well radius	0.15 m
Injection rate	8.87 kg/s (1,600 m^3/d)
Capillary pressure, p_c	–
Distance between wells	100 m
Dimensions of model domain	1,000 × 1,000 × 160 m
Simulation time, t	1,000 days

2.2.2 Numerical scheme

The partial differential equations in Eq. 1 are discretized in space using the so-called Box method [13], which is a vertex-centered finite volume method. The finite volume mesh is constructed by discretizing the domain with a finite element mesh consisting of arbitrary element types and then connecting the element barycenters with edge barycenters to obtain a dual mesh of control volumes (see figure 3). The primary variables are calculated on the corners of the finite element mesh, and linear shape functions are used to interpolate their values between the nodes. The Box method is locally mass-conservative. The mobilities are fully upwinded. Time discretization is done with an implicit Euler scheme. The non-linear system is linearized using a Newton–Raphson method. As mentioned earlier, the numerical scheme is implemented in the numerical simulator MUFTE-UG. Details concerning the numerical algorithms, for example, multigrid methods, parallelization, etc., can be found in [2] and [6].

2.2.3 Model domain

Much of the domain (including the domain dimensions, the positions of the aquifers and the CO_2 injection rate) has been described in Section 2.1.1 and in figure 2. The leaky well is located at the center of the domain. In the semi-analytical solution, the injection well is taken to be the center of the domain. The aquitard between the two aquifers is completely impermeable, and for computational efficiency, only the aquifers and the leaky well are meshed. The boundaries between the meshed regions and the aquitard are taken to be no-flow

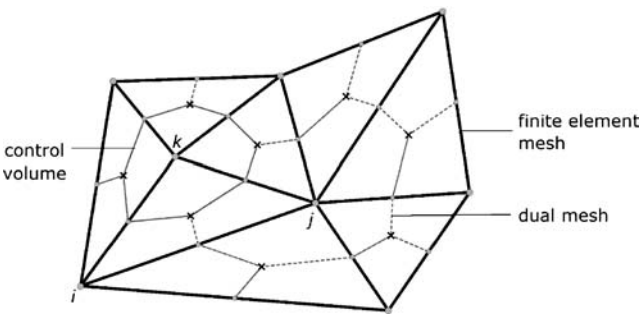

Figure 3 Finite element mesh and dual mesh constructed to be used as control volumes (from [7]).

boundaries. The aquifers are initially saturated with brine, and the pressure is hydrostatic ($\nabla p_z = \varrho_w \cdot g = 1,045\,\mathrm{kg/m^3} \cdot 9.81\,\mathrm{m/s^2} = 10,251.145\,\mathrm{Pa/m}$) with $p = 2.921 \times 10^7\,\mathrm{Pa}$ at the top of the domain (at 2,840 m depth). These conditions are also the lateral boundary conditions (Dirichlet). At the top and bottom of the domain, there are no-flow boundary conditions (Neumann) for both brine and CO_2. None of the boundary conditions changes with time.

The mesh (with 65,985 nodes) is made up of tetrahedra of varying sizes. Near the injection and leaky wells, the mesh is fine and gets coarser towards the boundaries. The mesh is also refined between the wells at the top of the lower aquifer to be able to better model the shape of the CO_2 plume between the wells, which has a strong effect on the CO_2 arrival time at the leaky well. The edge length of the elements ranges from 0.267 m at the wells to 15 m at the lateral boundaries. The wells are discretized as having a square cross-sectional area ($0.267 \times 0.267\,\mathrm{m}$) equal to that of a circular cross-section with a radius of 0.15 m. Figure 4 shows the bottom view of the mesh, and figure 5 depicts the mesh on a vertical slice through the middle of the domain. In both figures, the refinement of the mesh around the wells can be seen. The mesh is, however, not considered fine enough to guarantee a converged solution. To get rough estimates of the error arising from this, a two-dimensional mesh convergence study has been carried out and is given in Appendix. For more general studies on the properties of the Box method with respect to the grid dependence of numerical solutions, see [16].

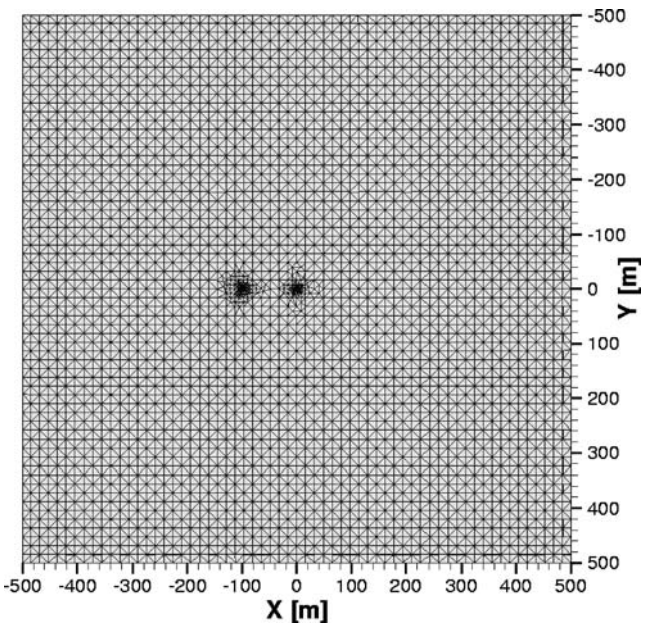

Figure 4 Bottom view of the mesh.

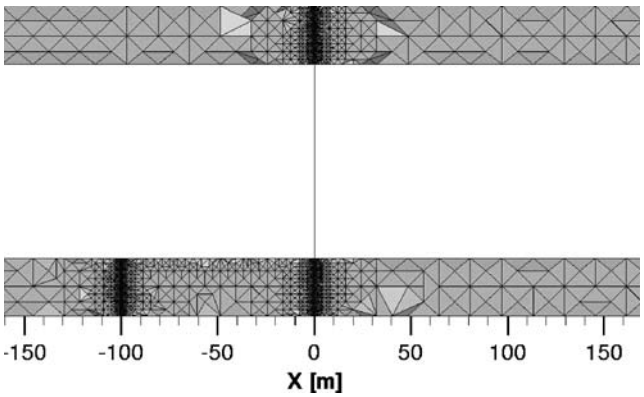

Figure 5 Vertical slice through the middle of the domain showing the mesh refinement around the wells and at the top of the lower aquifer between the wells.

2.2.4 Results

Figure 6 shows the distribution of the CO_2 saturation and pressure on a slice through the middle of the domain after 80 days of injection. The CO_2 spreads radially from the injection well and, upon reaching the leaky well, rises to the higher aquifer.

2.3 Comparison of numerical and semi-analytical results

The leakage rates as a function of time for the semi-analytical solution by Nordbotten et al. and the numerical simulation using MUFTE-UG are shown in figure 7. In the numerical simulation, leakage is calculated as the CO_2 flux at the middle of the leaky well ($z = 80\,\mathrm{m}$, see figures 2 and 6). This differs a bit from the method used in the computation of leakage in the semi-analytical solution, which is done by calculating the flux using values for pressure and saturation at the top and bottom of

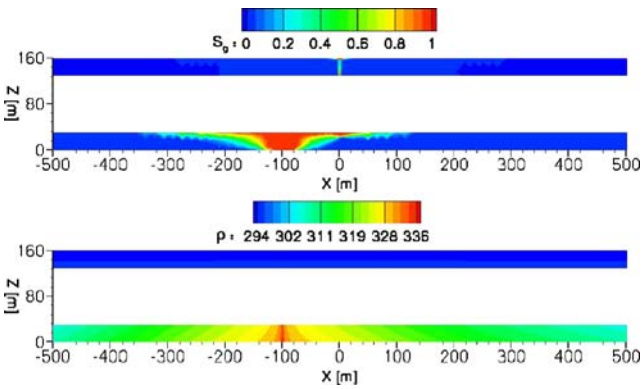

Figure 6 Numerical results: CO_2 saturation (*top*) and pressure in bar (*bottom*) at $t = 80$ days.

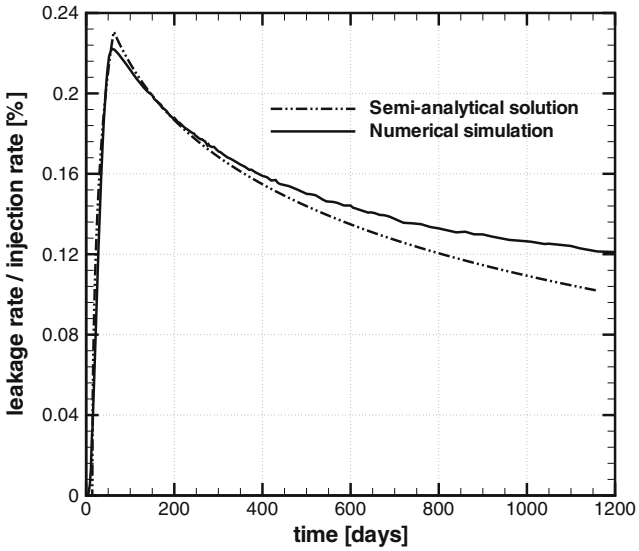

Figure 7 Leakage rate through the leaky well – semi-analytical solution and numerical simulation.

the leaky well. This is, however, not expected to have a strong effect on the results.

The CO_2 flux in the leaky well rises sharply when the CO_2 reaches the well and then drops. This drop in the leakage rate can be attributed to the lateral boundary conditions that influence the pressure in the domain. For an infinitely large domain, the CO_2 flux would not be expected to drop but to continue increasing slowly after the initial sharp rise [21]. In table 2, the leakage values (which are calculated as the leakage rates divided by the injection rate in percent) at the peak of the curve and at $t = 1,000$ days are given. The time at which the CO_2 plume reaches the well (which is defined as the time at which the leakage value is greater than 5.0×10^{-3} %) is also given in the table.

The two results differ for late times. This difference is attributed to the different positions the leaky and injection wells have in the two different methods. For the numerical simulation, the leaky well is in the center of the domain, whereas the semi-analytical solution takes the injection well to be the center of the domain. This implies that the boundary effects on the pressure at the bottom of the leaky well are less for the numerical simulation.

The early arrival time of the CO_2 at the leaky well in the numerical simulation is in part due to grid effects. The mesh convergence study in Appendix shows that one would obtain a slightly later CO_2 arrival with a finer mesh.

2.3.1 Variation of the reference problem

An interesting variation of the reference problem is the use of non-linear relative permeability–saturation relations and the introduction of residual saturations as well as capillary pressure. The pressures in the brine phase and in the gas phase then differ by the capillary pressure ($p_g = p_w + p_c$). Thus, Eq. 1 has to be modified to differentiate between the two pressures.

The effect these changes have on the leakage rate is investigated in this section. The relative permeability–saturation and capillary pressure–saturation relations [5] used are given in table 3. All other parameters and assumptions remain the same as in the reference problem described previously.

The leakage rates for the reference problem and its variation are shown in figure 8. The linear relative permeability–saturation relations used in the reference case imply that the sum of the relative permeability values of the brine and gas phases is equal to unity for any given saturation. In the variation, this sum is less than unity for most saturations. As a result of this increased overall resistance to flow, the leakage rate does not rise as high as in the reference case. The lower relative permeabilities also increase the influence of the viscous forces in the system (compared to buoyancy) making the shape of the plume become more cylindrical than in the reference case (compare figure 9 to figure 6). This leads to the later arrival time of CO_2 at the leaky well. However, at late times, the two curves converge to similar leakage rates.

Table 2 Comparison of the semi-analytical solution by Nordbotten et al. and the results of the numerical simulation using MUFTE-UG.

	Semi-analytical solution	Numerical simulation
Approx. arrival time of the CO_2 at the leaky well [days]	14	8
Maximum leakage value (leakage flux/injection rate) [%]	0.231	0.222
Leakage value at $t = 1,000$ days (leakage flux/injection rate) [%]	0.109	0.126

Table 3 Changed functions/parameters.

Parameter	Value/function
Residual brine saturation, S_{wr}	0.2
Residual gas saturation, S_{gr}	0.05
Capillary pressure, p_c	$p_c = p_d S_e^{-\frac{1}{\lambda}};\ p_c \geq p_d$
Brine phase relative permeability, k_{rw}	$k_{rw} = S_e^{\frac{2+3\lambda}{\lambda}}$
Gas phase relative permeability, k_{rg}	$k_{rg} = (1 - S_e)^2 \left(1 - S_e^{\frac{2+\lambda}{\lambda}}\right)$
Effective saturation, S_e	$S_e = \frac{S_w - S_{wr}}{1 - S_{wr} - S_{gr}};\ S_{wr} \leq S_w \leq 1 - S_{gr}$
Entry pressure, p_d	10^4 Pa
Brooks–Corey parameter, λ	2.0

3 The non-isothermal two-phase two-component problem including compositional effects

In the leakage scenario defined in Section 2.1.1, the aquifer is very deep, and pressure and temperature are very high. At such conditions, CO_2 is supercritical and there are no abrupt changes with depth in the fluid properties (density, viscosity and enthalpy) of CO_2. This leads to the assumption of constant and average CO_2 fluid properties. In this section, leakage at shallow depths (640 to 800 m) will be considered. Figure 11 shows the pressure and temperature in the formation at the mentioned depths (assuming a geothermal gradient of 0.03 K/m). The conditions in the aquifer at the considered depths range from supercritical to liquid to gaseous (see figure 10). In figure 11, the density CO_2 would have at the conditions in the formation is shown. There is a large change in density at a certain depth. This depth corresponds to the point where the line depicting the formation conditions crosses the CO_2 saturation vapor curve, that is, the boundary between liquid and gaseous CO_2. Other physical properties such as viscosity and enthalpy would also change abruptly at that depth. Obviously, the numerical model discussed in Section 2.2 needs to be extended to account for such effects. It also needs to account for the dissolution of CO_2 in brine, as this has an effect on the leakage rate.

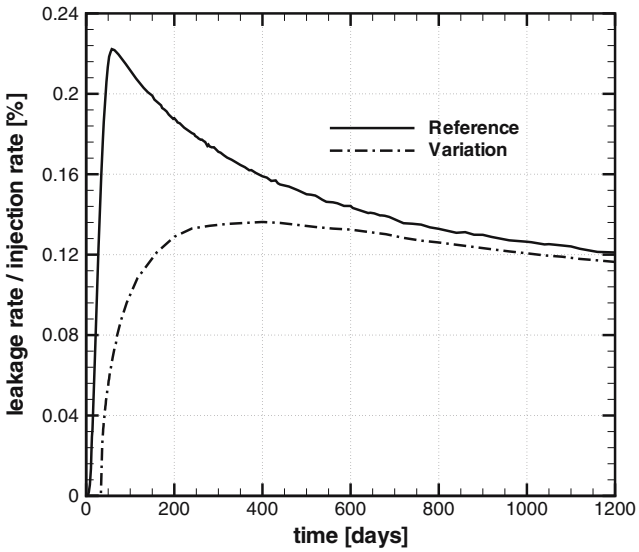

Figure 8 Leakage rate through the leaky well for the numerical reference problem (linear relative permeability–saturation relations, no capillary pressure) and the variation (non-linear relative permeability–saturation and capillary pressure–saturation relations).

3.1 Extended model concept

In this section, a non-isothermal two-phase two-component model concept is used to describe the flow processes of the leakage problem in more physical detail. Two phases are modeled – brine and gas. The brine phase is made up of two components (CO_2 and water). Thus, CO_2 from the gas phase can dissolve in the brine phase. Dissolution of water in the gas phase is neglected – the gas phase contains only one component. Salinity is taken to be a constant parameter that affects the fluid properties of the brine phase and the amount of dissolved CO_2 (salting out). The model concept also accounts for thermal processes that may occur while the CO_2 migrates through the formation. The two mass balance equations for each of the components κ (water and CO_2) are given in Eq. 3, where α stands for the phase (brine w or gas g), X_α^κ is the mass fraction of the

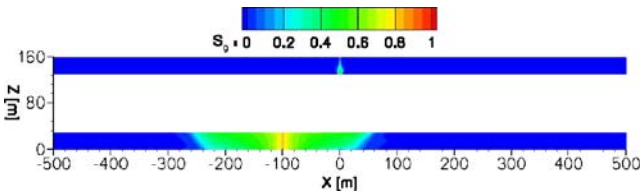

Figure 9 Numerical results: CO_2 saturation $t = 80$ days for the variation.

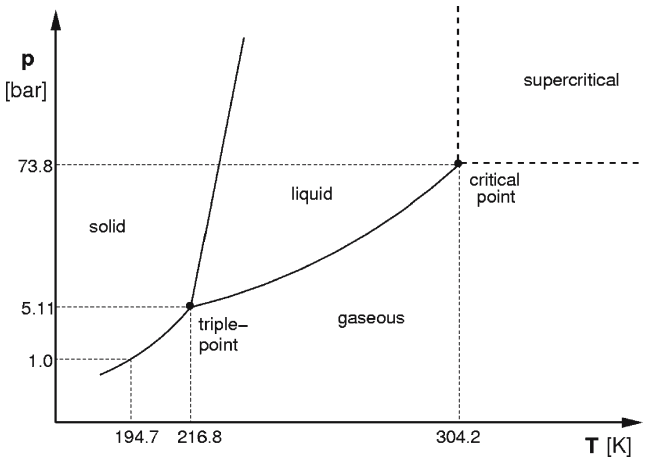

Figure 10 Phase diagram of CO_2.

component κ in the phase α and $D_{\mathrm{pm}}^{\mathrm{CO2}}$ is the diffusion coefficient of CO_2 in the porous medium.

$$\phi \frac{\partial \left(\sum_\alpha \varrho_\alpha X_\alpha^\kappa S_\alpha\right)}{\partial t} - \sum_\alpha \nabla \cdot \left\{\lambda_\alpha \varrho_\alpha X_\alpha^\kappa \mathbf{K}(\nabla p_\alpha - \varrho_\alpha \mathbf{g})\right\} - \nabla \cdot \left\{D_{\mathrm{pm}}^{\mathrm{CO2}} \varrho_{\mathrm{w}} \nabla X_{\mathrm{w}}^\kappa\right\} - q^\kappa = 0;$$
$$\kappa \in \{\mathrm{w}, \mathrm{CO2}\}, \quad \alpha \in \{\mathrm{w}, \mathrm{g}\}. \tag{3}$$

Energy balance equations are necessary for modeling temperature changes. Under the assumption of local thermal equilibrium, only one energy balance equation for the fluid-filled porous medium is necessary (Eq. 4).

$$\phi \frac{\partial \left(\sum_\alpha \varrho_\alpha u_\alpha S_\alpha\right)}{\partial t} + (1-\phi) \frac{\partial (\varrho_{\mathrm{s}} c_{\mathrm{s}} T)}{\partial t} - \nabla \cdot \left(\lambda_{\mathrm{pm}} \nabla T\right) - \sum_\alpha \nabla \cdot \left\{\lambda_\alpha \varrho_\alpha h_\alpha \mathbf{K}\left(\nabla p_\alpha - \varrho_\alpha \mathbf{g}\right)\right\} - q^h = 0;$$
$$\alpha \in \{\mathrm{w}, \mathrm{g}\}. \tag{4}$$

T stands for temperature, u is the specific internal energy (J/kg), ϱ_{s} and c_{s} are the density (kg/m^3) and the specific heat capacity [J/(kg K)] of the porous medium, respectively, λ_{pm} is the effective heat conductivity [W/(m^2 K)] of the fluid-filled porous medium and h stands for specific enthalpy (J/kg). Eqs. 3 and 4 are constrained by the following equations.

$$p_{\mathrm{w}} + p_{\mathrm{c}}(S_{\mathrm{w}}) = p_{\mathrm{g}} \tag{5}$$
$$S_{\mathrm{w}} + S_{\mathrm{g}} = 1 \tag{6}$$
$$\sum_\kappa X_\alpha^\kappa = 1 \tag{7}$$

An overview of the fluid properties of CO_2 and brine as used in the model is given in table 4. Details of the model concept can be found in [4] .

3.1.1 Model domain and parameters

The domain used in this simulation is similar to the one used in Section 2. In this case, however, the domain is located between 640 and 800 m below the surface. The simulation parameters that differ from those of table 1 are given in table 5. Note that the injection rate is given as a constant CO_2 mass flux. This does not imply that the volume flux of CO_2 is constant as was the case in Section 2 because the CO_2 density now varies with temperature and pressure. The relative permeabilities and capillary pressure are treated as discussed in Section 2.3.1.

The mesh used in this section differs slightly from the one used previously. In Section 2, the aquitard was completely cut out of the mesh and not modeled. To be able to model temperature changes in the leaky well, a 10 × 10 m region of the aquitard around the leaky well is meshed and included in the simulation. This region is included around the well to model the heat exchange between the well and the aquitard due to heat

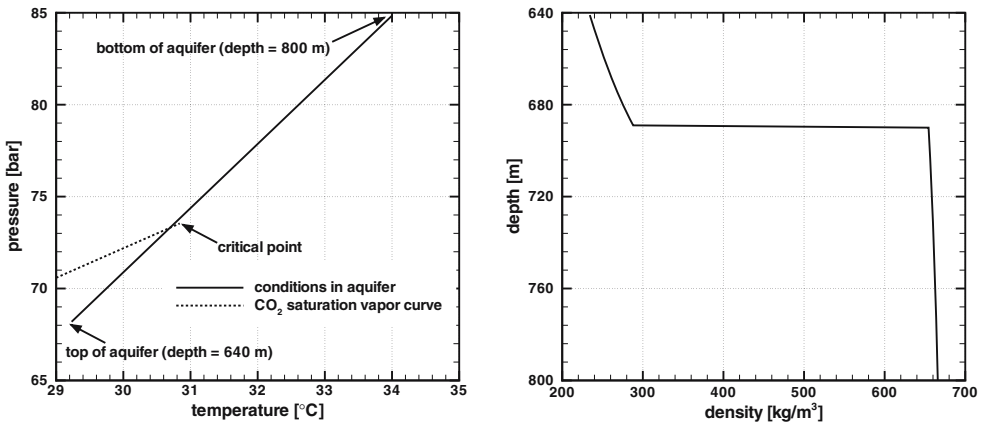

Figure 11 Pressure and temperature conditions in the formation (*left*), density of CO_2 with depth (*right*).

Table 4 Fluid properties of CO_2 and brine.

Fluid property	Function of	Literature
CO_2 density, ϱ_g	$f(T, p)$	Span and Wagner [26]
CO_2 enthalpy, h_g	$f(T, p)$	Span and Wagner [26]
CO_2 viscosity, μ_g	$f(T, p)$	Fenghour et al. [10]
Brine density, ϱ_w	$f(T, p, S, X_w^{CO2})$	Batzle and Wang [3], Garcia [11], IAPWS [17]
Brine enthalpy, h_w	$f(T, p, S, X_w^{CO2})$	Daubert and Danner [8] , Duan and Sun [9], IAPWS [17], Michaelides [18]
Brine viscosity, μ_w	$f(T, S)$	Batzle and Wang [3]

conduction. A cross-section of the leaky well with the included region around it and the mesh can be seen in figure 12. The modeled part of the aquitard is assigned a permeability of $1 \times 10^{-18}\,m^2$.

3.1.2 Discussion of the results

Figure 13 shows the leakage rate as a function of time; the distribution of CO_2 saturation on a vertical slice through the middle of the domain at $t = 80$ days is shown in figure 14. A quantitative comparison of the results obtained in this extended model problem and those of the reference problem (Section 2.1.1) is not our focus because the two cases differ in too many ways (parameters, boundary and initial conditions, model concept, etc.). One can, however, state qualitatively the influence of these differences, as is done in the following.

- In Section 2.3.1, the influence of the implemented non-linear relative permeability–saturation relations on the leakage rate and on the shape of the plume was discussed. The same principle holds in this case.
- The injection rate in the extended model problem is given as a constant mass flux (table 5), which corresponds to that of the reference case (table 1). As a result of the difference in CO_2 density in the two cases (reference: $\varrho_g = 479\,kg/m^3$; extended model: $\varrho_g \approx 665\,kg/m^3$), the volume flux and hence the leakage rate in the extended model problem are lower than in the reference problem.
- The compressibility of the fluids (especially CO_2) in the extended model has a lowering effect on the pressure build-up in the aquifer. This in turn lowers the leakage rate.
- The shape of the CO_2 plume in the lower aquifer is determined by the interplay of viscous forces and buoyancy. The high density in the extended model case reduces buoyancy. The viscous forces, on the other hand, are greater than in the reference case because of the higher viscosities (reference: $\mu_g = 3.95\times10^{-5}$ Pa s, $\mu_w = 2.54\times10^{-4}$ Pa s; extended model: $\mu_g \approx 8.20\times10^{-5}$ Pa s, $\mu_g \approx 9.87\times10^{-4}$ Pa s) and thus higher resistance to flow. The resulting shape of the plume is cylindrical (figure 14).

Table 5 Simulation parameters.

Parameter	Value
Injection rate	8.87 kg/s
Brine salinity, S	0.1 kg/kg
Geothermal gradient	0.03 K/m
Diffusion coefficient[1], D_w^{CO2}	$2.0 \times 10^{-9}\,m^2/s$
Simulation time, t	2,000 days

[1] $D_{pm}^{CO2} = \tau\phi S_w D_w^{CO2}$; τ is the tortuosity of the porous medium.

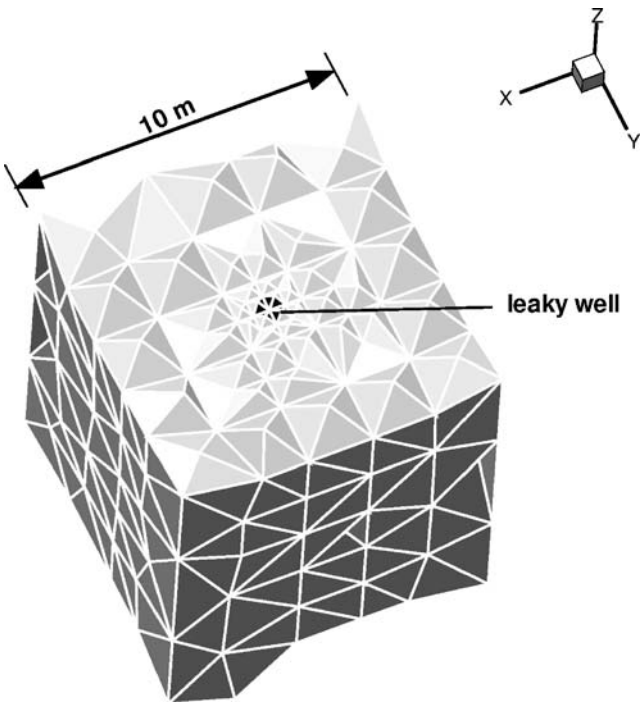

Figure 12 Cross-section of the leaky well with the included region of the aquitard.

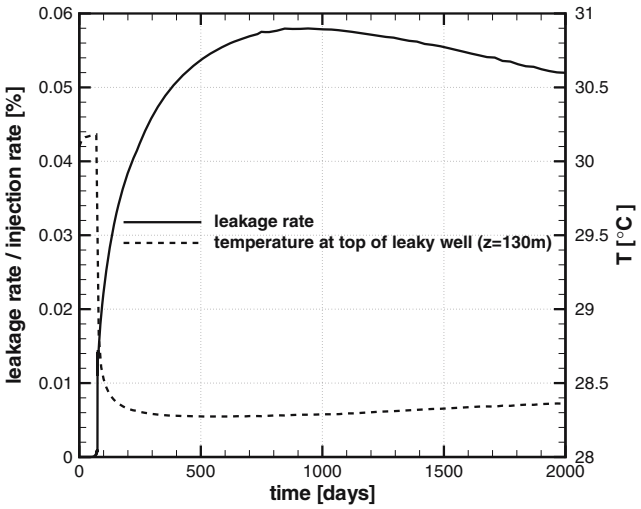

Figure 13 The *continuous line* shows the CO_2 leakage rate through the leaky well. The *dashed line* shows the temperature at the top of the leaky well ($z = 130$ m, see figures 2 and 6).

- Within the simulation time $70 < t < 2,000$ days, 7–10 % of the total mass of CO_2 in the model domain is dissolved in the formation brine, which implies a reduced amount of leaking CO_2 compared to the reference case.
- All the effects discussed above increase the arrival time of the CO_2 plume at the leaky well.

Figure 13 also shows the temperature at the top of the leaky well ($z = 130$ m, see figures 2 and 6). The temperature rises a bit as warm brine from lower regions in the formation flows upwards. There is a sudden temperature drop (when CO_2-rich phase reaches the top of the well), which is as a result of the phase change of the CO_2 (liquid to gas) in that region and the accompanying enthalpy changes. The temperature changes in this simulation are not very large, and their influence on the leakage rate is marginal. It has, however, been shown that for some CO_2 leakage cases, thermal effects can be very important with respect to leakage, as strong cooling can cause freezing of water or formation of gas hydrates [23].

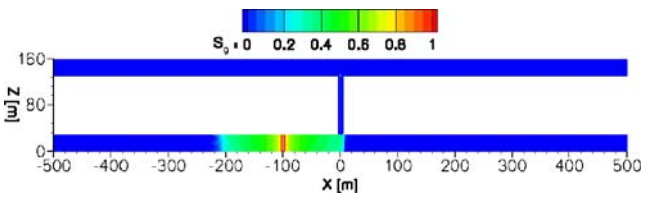

Figure 14 Numerical results: CO_2 saturation $t = 80$ days for the extended model problem.

4 Summary and conclusions

This benchmark study addresses the problem of well leakage during CO_2 injection into a saline aquifer. The physical background is motivated by the huge number of abandoned wells penetrating possible target formations for the storage of CO_2, particularly in North American sedimentary basins where oil and gas production activities provide an already existing infrastructure. The demand for new benchmark studies grows because of the intensive development of sophisticated models and a lack of reliable and controlled experimental data for validation.

The benchmarks are aimed to provide a basis for the intercomparison of analytical and numerical models with respect to problem-oriented questions. In the present study, this concerns mainly the development of the leakage rate over time, the evolution of the plume in the aquifers and the arrival time of the CO_2 at the leaky well. Different model concepts generally do not use the same assumptions, simplifications and approaches. Thus, the deviations in the results allow a qualitative and quantitative evaluation of the respective parameters and processes that are specific for a model. We show in Section 2 that the best-possible adaption of the numerical model parameters to those of the semi-analytical solution can reproduce the leakage rates very well, particularly the peak rate. The deviation in the tailing reveals the influence of a slightly different assignment of the boundary conditions, which is due to the fact that the domains are not fully identical in both models. Concerning the arrival time of the plume at the leaky well, the comparison with the semi-analytical solution shows, as could be expected due to numerical diffusion and shown in Appendix, an overestimation of the plume propagation. One could reduce the error due to numerical diffusion by the use of adaptively refined grids.

Section 3 describes the same principle benchmark example, but with less restrictions and simplifying assumptions. Non-isothermal and compositional effects are taken into account, and the problem now takes place in a depth where the leaky well intersects the critical depth at which the CO_2 would lose its supercritical state of aggregation. No analytical approaches are available for this degree of complexity, and the implementation of numerical codes for modeling such a problem may differ with respect to the calculation of sub- and supercritical fluid properties, phase composition, discretization methods, etc. We therefore propose the use of this benchmark example to other modelers to test their models and compare results.

It is evident that the semi-analytical reference solutions for this kind of problem can efficiently provide reasonable estimates for the leakage rates and arrival times of the plume at a potentially leaking well. The advective transport of the CO_2 due to the injection pressure and the density difference is the major mechanism for the occurring leakage. The more detailed inclusion of physical processes by the non-isothermal two-phase two-component model revealed that the leakage rate obtained with the semi-analytical solution procedure appears to be a conservative estimate because the neglected processes are leakage-mitigating. The semi-analytical model cannot account for more detailed aspects like the temperature changes because of the rapid expansion of the CO_2 in the leaky well as shown in this work. This holds also for other aspects of CO_2 storage; for example, the investigation of storage mechanisms, where the density variations of CO_2 enriched brine, and the thereby induced advective and diffusive transport play an important role because they favor the long-term storage in the formation (see [4]). Thus, for improving the understanding of the coupled non-linear processes, the sophisticated multicomponent model concept is an indispensable tool.

Both semi-analytical and numerical models agree on a decrease of the leakage rates after reaching a certain peak value. We must note that this crucially depends on the distance of the Dirichlet boundary condition for the pressure in the lower aquifer. The farther away this Dirichlet condition from the injection well, the more pressure can build up at the wells with the result of further increased leakage. Even worse would be a situation where the storage formation is confined by an impermeable barrier so that pressure build-up is further favored. Any specific real formation has to be evaluated with respect to the boundary condition assumed in this study before transferring its results to a specific site. There are also factors that can mitigate the pressure increase, for example, the compressibility/elasticity of the rocks. The implementation of equations accounting for the geomechanical behavior is necessary to study this topic more closely.

Eventually, the assessment of potential leakage risks through abandoned wells requires a thorough understanding of the physical processes and mechanisms. Studying those with models and benchmark problems as presented here contributes towards reaching that goal. The same holds for the large number of other aspects that have to be investigated such as storage capacities or the injection into other than saline aquifer formations. Within the current project, in the frame of which this study was performed, we plan to define further problem-oriented benchmarks concerned with storage mechanisms, enhanced methane (CH_4) recovery by CO_2 injection and sorption of CO_2 and CH_4.

Acknowledgements The authors particularly thank Dr Jan Nordbotten from the University of Bergen/Norway for his generous collaboration. This is publication no. GEOTECH-243 of the R&D-Program GEOTECHNOLOGIEN funded by the German Ministry of Education and Research (BMBF) and German Research Foundation (DFG), Grant (Förderkennzeichen) 03G0620A.

Appendix

Two-dimensional mesh convergence study

Because of computation time limitations, mesh convergence of the numerical simulations on the large three-

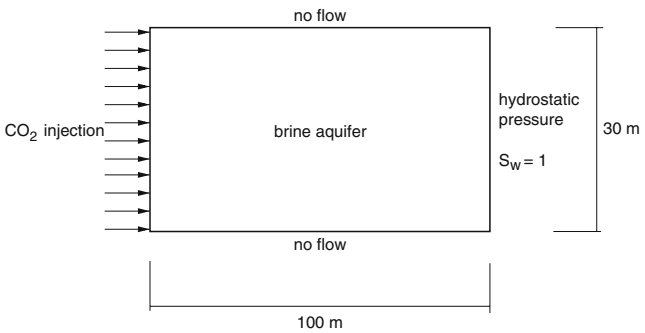

Figure 15 Model set-up used in the convergence study.

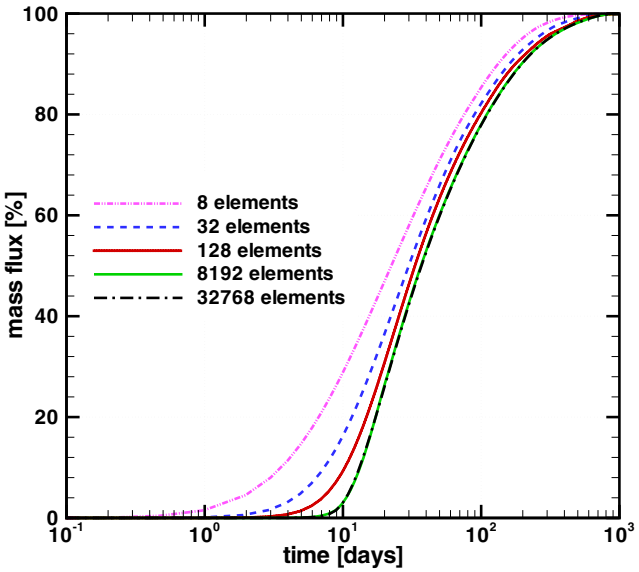

Figure 16 Convergence of the solution for the mass flux over the right domain boundary.

dimensional mesh could not be investigated. However, to get an idea of how the grid effects could alter the solutions, grid convergence on a two-dimensional grid is examined. The rectangular x–z-plane between the injection and leaky well is taken as the simulation domain. CO_2 is injected over the left boundary of the domain, and the pressure and saturation conditions on the right boundary are kept constant as shown in figure 15. The fluid and aquifer properties are the same as in the reference case described in Section 2.1.1. The injection rate is chosen to be 0.03 kg/ms, which gives a similar plume shape as in Section 2.2.4. The domain is meshed uniformly with triangles. For the first simulation, the domain is discretized with eight elements, and the mass flux over the right boundary is computed. The number of elements is increased until the solution converges. In figure 16, the mass flux expressed as a fraction of the injection rate over time is shown. Note that the time scale is logarithmic.

From figure 16, one can deduce the following.

- The arrival time of the CO_2 at the right boundary increases with increasing number of elements. This would imply that the arrival time given in table 2 is probably underestimated.
- Simulations on coarse grids generally overestimate the flux.
- The error reduces with simulation time.

References

1. Assteerawatt, A., Bastian, P., Bielinski, A., Breiting, T., Class, H., Ebigbo, A., Eichel, H., Freiboth, S., Helmig, R., Kopp, A., Niessner, J., Ochs, S.O., Papafotiou, A., Paul, M., Sheta, H., Werner, D., Ölmann, U.: MUFTE-UG: structure, applications and numerical methods. Newsletter, International Groundwater Modeling Centre, Colorado School of Mines **23**(2), (10/2005)
2. Bastian, P., Helmig, R.: Efficient fully-coupled solution techniques for two phase flow in porous media. Parallel multigrid solution and large scale computations. Adv. Water Resour. **23**, 199–216 (1999)
3. Batzle, M., Wang, Z.: Seismic properties of pore fluids. Geophysics **57**, 1396–1408 (1992)
4. Bielinski, A.: Numerical simulation of CO_2 sequestration in geological formations. PhD thesis, Universität Stuttgart (2006)
5. Brooks, A.N., Corey, A.T.: Hydraulic properties of porous media. In: Hydrol. Pap. Fort Collins, Colorado State University (1964)
6. Class, H., Helmig, R., Bastian, P.: Numerical simulation of non-isothermal multiphase multicomponent processes in porous media. – 1. An efficient solution technique. Adv. Water Resour. **25**, 533–550 (2002)
7. Class, H., Helmig, R., Niessner, J., Ölmann, U.: Multiphase Processes in Porous Media, Multifield Problems in Solid and Fluid Mechanics, 28th edition, pp. 45–82. Springer, Berlin Heidelberg New York (2006)
8. Daubert, T.E., Danner, R.P.: Physical and thermodynamic properties of pure chemicals: data compilation. Design Institute for Physical Property Data (1989)
9. Duan, Z., Sun, R.: An improved model calculating CO_2 solubility in pure water and aqueous NaCl solutions from 273 to 533 K and from 0 to 2000 bar. Chem. Geol. **193**, 257–271 (2003)
10. Fenghour, A., Wakeham, W., Vesovic, V.: The viscosity of carbon dioxide. J. Phys. Chem. Ref. Data **27**(1), 31–44 (1998)
11. Garcia, J.: Density of aqueous solutions of CO_2. Technical report, LBNL Report 49023, Lawrence Berkeley National Laboratory, Berkeley, CA, USA (2001)
12. Gasda, S., Bachu, S., Celia, M.: Spatial characterization of the location of potentially leaky wells penetrating a deep saline aquifer in a mature sedimentary basin. Environ. Geol. **46**, 707–720 (2004)
13. Helmig, R.: Multiphase Flow and Transport Processes in the Subsurface. Springer, Berlin Heidelberg New York (1997)
14. Helmig, R., Class, H., Huber, R., Sheta, H., Ewing, R., Hinkelmann, R., Jakobs, H., Bastian, P.: Architecture of the modular program system MUFTE-UG for simulating multiphase flow and transport processes in heterogeneous porous media. Math. Geol. **2**, 123–131 (1998)
15. Holloway, S.: Storage of fossil fuels-derived carbon dioxide beneath the surface of the earth. Ann. Rev. Energy Environ. **26**, 145–166 (2001)
16. Huber, R., Helmig, R.: Node-centered finite-volume discretization for the numerical simulation of multiphase flow in heterogeneous porous media. Comput. Geosci. **4**, 141–164 (2000)
17. IAPWS: Release on the IAPWS Industrial Formulation 1997 for the Thermodynamic Properties of Water and Steam. The International Association for the Properties of Water and Steam (1997) http://www.iapws.org/.
18. Michaelides, E.: Thermodynamic properties of geothermal fluids. Geotherm. Resour. Counc. Trans. **5**, 361–364 (1981)
19. Nordbotten, J., Celia, M., Bachu, S.: Analytical solutions for leakage rates through abandoned wells. Water Resour. Res. **40**(4), W04204 (2004)
20. Nordbotten, J., Celia, M., Bachu, S.: Injection and storage of CO_2 in deep saline aquifers: analytical solution for CO_2 plume evolution during injection. Transp. Porous Media **58**(3), 339–360 (2005a)
21. Nordbotten, J., Celia, M., Bachu, S., Dahle, H.: Semi-analytical solution for CO_2 leakage through an abandoned well. Environ. Sci. Technol. **39**(2), 602–611 (2005b)
22. Oldenburg, C., Pruess, K., Benson, S.: Process modeling of CO_2 injection into natural gas reservoirs for Carbon sequestration and enhanced gas recovery. Energy Fuels **15**(2), 293–298 (2001)
23. Pruess, K.: Thermal effects during CO_2 leakage from a geologic storage reservoir. Lawrence Berkeley National Laboratory Report LBNL-55913 (2004)
24. Pruess, K., Bielinski, A., Ennis-King, J., Fabriol, R., Le Gallo, Y., Garcia, J., Jessen, K., Kovscek, T., Law, D.-S., Lichtner, P., Oldenburg, C., Pawar, R., Rutqvist, J., Steefel, C., Travis, B., Tsang, C.-F., White, S., Xu, T.: Code intercomparison builds confidence in numerical models for geologic disposal of CO_2 . In: Gale, J., Kaya, Y. (eds.) GHGT-6

Conference Proceedings: Greenhouse Gas Control Technologies, pp. 463–470 (2003)
25. Pruess, K., Garcia, J.: Multiphase flow dynamics during CO2 injection into saline aquifers. Environ. Geol. **42**, 282–295 (2002)
26. Span, R., Wagner, W.: A new equation of state for carbon dioxide covering the fluid region from the triple-point temperature to 1100 K at pressures up to 800 MPa. J. Phys. Chem. Ref. Data **25**(6), 1509–1596 (1996)